



City Research Online

City, University of London Institutional Repository

Citation: Rane, S., Kovacevic, A., Stosic, N. & Smith, I. (2021). Analysis of real gas equation of state for CFD modelling of twin screw expanders with R245fa, R290, R1336mzz(Z) and R1233zd(E). *International Journal of Refrigeration*, 121, pp. 313-326. doi: 10.1016/j.ijrefrig.2020.10.022

This is the accepted version of the paper.

This version of the publication may differ from the final published version.

Permanent repository link: <https://openaccess.city.ac.uk/id/eprint/25590/>

Link to published version: <https://doi.org/10.1016/j.ijrefrig.2020.10.022>

Copyright: City Research Online aims to make research outputs of City, University of London available to a wider audience. Copyright and Moral Rights remain with the author(s) and/or copyright holders. URLs from City Research Online may be freely distributed and linked to.

Reuse: Copies of full items can be used for personal research or study, educational, or not-for-profit purposes without prior permission or charge. Provided that the authors, title and full bibliographic details are credited, a hyperlink and/or URL is given for the original metadata page and the content is not changed in any way.

City Research Online:

<http://openaccess.city.ac.uk/>

publications@city.ac.uk

Analysis of Real Gas Equation of State for CFD Modelling of Twin Screw Expanders with R245fa, R290, R1336mzz(Z) and R1233zd(E)

Sham Rane*, Ahmed Kovačević, Nikola Stošić, Ian Smith

City, University of London, London, EC1V 0HB, UK

*Corresponding Author: sham.rane@city.ac.uk, tel: +44 (0) 20 70408795

ABSTRACT

Positive displacement expanders are widely investigated and their models commonly use the REFPROP database to evaluate fluid properties. However, estimating procedures in CFD models using REFPROP result in heavy use of CPU time. Therefore, a study has been carried out to determine if simpler methods for fluid property estimation are suitable. The ANSYS CFX solver used includes a number of cubic equations of state, namely, the Redlich Kwong, Soave Redlich Kwong, Aungier Redlich Kwong and Peng Robinson. To determine their suitability, performance simulations were carried out with each of them, on a twin screw expander with a 4/5 rotor configuration and an “N” rotor profile, operating with R245fa, R290, R1336mzz(Z) and R1233zd(E). For each considered equation, the expander’s performance results deviation from those obtained using REFPROP is evaluated. These results show that the ideal gas equation of state gives predictions of flow and power that deviate significantly from those determined with REFPROP. The alternatively available cubic equations give far better agreement. Of these, the RK equation has the highest deviation, although it differs by only 2.2% maximum from the REFPROP values. The PR equation yields the closest agreement with a deviation of the order of only 0.8%, while the deviation with both SRK and ARK equations is less than 1.1% maximum, practically negligible. Apart from the good agreement obtained, the use of the real gas equations, in place of REFPROP, resulted in a saving of approximately 43% in CPU operating time to obtain same level of convergence of the solver.

Keywords: Twin Screw Expander CFD; R245fa; R1336mzz(Z); R1233zd(E); Real Gas Cubic Equation of State; REFPROP

NOMENCLATURE

a, b	equation of state model parameters	P	indicated power
a_0, b_0, c_0	model constants	R	molar gas constant (8.314472 J mol ⁻¹ K ⁻¹)
c_p	specific heat (J kg ⁻¹ K ⁻¹)	R_s	specific gas constant (J kg ⁻¹ K ⁻¹)
\dot{m}	mass flow rate	T	temperature (K)
M	molecular weight (g mol ⁻¹)	V_i	built-in volume index
p	pressure (Pa)		
α	temperature function	ρ	density
λ	thermal conductivity	σ	collision diameter
μ	dynamic viscosity	ω	acentric factor
v	specific volume (kg m ⁻³)	Ω	collision function

Subscripts

$0, 1, 2, 3, 4$	model constants	s	specific fluid property
c	critical conditions	r	reference quantity
p	at constant pressure	v	at constant volume

Abbreviations

ARK	Aungier Redlich Kwong	REFPROP	Reference Fluid Thermodynamic and Transport Properties Database
CFD	Computational Fluid Dynamics	RK	Redlich Kwong
NIST	National Institute of Standards and Technology	SCORG	Screw Compressor Rotor Grid Generator
PR	Peng Robinson	SRK	Soave Redlich Kwong

1. Introduction

As an alternative to turbines, volumetric machines are being widely used to expand organic working fluids in Rankine cycle (ORC) systems for power generation in the 3 to 50 kW range. Typically, these systems are used for waste heat recovery from industrial processes or as bottoming cycle of a primary Rankine cycle steam power plant (Smith, 1993). For heat sources at lower temperatures of up to 200°C, fluids such as R134a (Tetrafluoroethane) or R245fa (1,1,1,3,3-Pentafluoropropane) or light hydrocarbons have a number of advantages over steam. These include, greater recoverable heat, due to their lower latent heat, and positive slope of the saturation line, when plotted on temperature-entropy coordinates, leading to dry vapour expansion resulting in higher expander efficiencies and higher power output. In addition, their considerably higher vapour pressures at condensing temperatures eliminate the problem of air leakage into the condenser and enable the expander to be much more compact, thus reducing costs.

The current research work is motivated from some of the results reported in recent literature on use of CFD models for performance evaluation of twin screw expanders used in ORC systems. Papeš et al. (2015) presented a CFD analysis of a 7 kW twin-screw expander in an ORC system with R245fa working fluid using ANSYS FLUENT solver. They tested alternative specifications of properties of R245fa using the ideal gas equation of state, the Aungier Redlich Kwong (ARK) equation of state and the CoolProp library. It was reported that the difference in power output between the ideal gas equation of state and the ARK equation of state was 8% and between ARK equation of state and CoolProp database was negligible for the operating conditions that were analysed. Along with this study, Abdelli (2015) in his thesis has reported analysis of the expansion process corresponding to the same twin-screw expander but with a simplified geometry with square cross section. Dynamic mesh using layering algorithm in ANSYS FLUENT solver was used for the volumetric expansion and piston linear motion. In the ORC operating conditions (0.1-2 MPa and 300-450°K), the ARK equation of state showed maximal pressure deviations of 15% comparing to CoolProp database. For specific heat, the deviations were a maximum of 10% for the ARK equation of state, while the ideal gas had a maximum of 30%. However, the relatively large deviations of the ARK equation results, only occurred very close to the saturated vapour line. The accuracy of the NIST REFPROP (Lemmon et al. 2018) and the CoolProp databases were identical. The 3D CFD calculations of twin-screw expander with 4-6 lobe, running at 6000 rpm, were performed for an expansion process from 0.6-0.1 MPa and 400-350°K. In these calculations with close to 2 million cell count, it was observed that the time required is twice when calculating with the CoolProp database as compared to ARK equation of state. It was not clear from this study, as to the level of solver convergence that was used for comparison or how the local variation of fluid properties within the expander differed.

In this paper, some of the cubic equation of state definitions available in the ANSYS CFX flow solver for dry real gas properties have been applied in the modelling of 3 kW twin-screw expander. The objective of this analysis was to evaluate computational accuracy in the prediction of expander performance and the flow solver's computational time requirements when using the real gas equation of state models compared to the property values derived from REFPROP. The expander modelled for this study had a 4-5 lobe combination, 'N' rotor profile and a built-in volumetric expansion ratio of 4.5 (Stošić et al., 2005). Its performance was evaluated at a filling pressure of 544 kPa at 94.26°C and a discharge pressure of 175 kPa (Bianchi et al., 2019). The grids generated for the rotors, expander chamber and high and low pressure ports were obtained using the SCORG software package. Observed differences in the CFD results have been reported in terms of the internal expansion pressure and temperature variation, mass flow rate, and indicated power output. Local variation of temperature and specific volume in the main and gate rotor chambers has been compared. Under the same operating condition, the results of the analyses were compared with those of the CFD model using REFPROP and the deviation in results are compared. An extended analysis was then carried out with R245fa and low GWP alternative working fluids R290 - (propane), R1336mzz(Z) - (trans-1-chloro-3,3,3-trifluoro-1-propene) and R1233zd(E) - (1,1,1,4,4,4-hexafluoro-2-butene), 1500 and 3000 rpm operating speed and 3.5 and 4.5 Vi. Wide variations in the test cases provide useful data for the validity of the observed results. R290 was evaluated at operating pressure of 600 kPa and temperature of 130.0°C while R1336mzz(Z) and R1233zd(E) were evaluated at operating pressure of 600 kPa and temperature of 110.0°C. Results from these test cases indicated that the real gas equations of state are a suitable alternative to specification of fluid properties in a 3D CFD model. The expander performance accuracy deviated within practically negligible limits of 1 – 1.5% and a consistent saving in computation time of the order of 43% was achievable.

The ideal gas equation of state overestimates pressure when applied for real gases, especially near the saturation line and critical point. The van der Waals equation of state was one of the first proposed for real gases in 1873. It modified the ideal gas equation of state by introducing terms associated with the finite size of the gas molecules and molecular attraction forces. The two main van der Waals modifications introduced to compensate for the pressure deviation were a reduction factor $v - b$ for specific volume and a reduction factor a/v^2 for pressure due to molecular attraction forces. These constants a and b have positive values and are a characteristic of each individual gas and assume a spherical shape of the molecules. The van der Waals equation of state reduces to the ideal gas equation of state when constants a and b are zero. The accuracy of the van der Waals equation of state was limited by keeping the values of a constant, since most molecules are non-spherical, while the value of b changes with pressure and temperature. Hence variations of this equation of state were developed in order to improve the accuracy and range of applicability. Some of these chronologically proposed are the Redlich Kwong in 1949, its variant the Soave Redlich Kwong in 1972, the Peng Robinson in 1976 and more recently the Aungier Redlich Kwong variant in 1995. These have all been included in this study.

1.1. Redlich Kwong Equation of State

Redlich and Kwong modified the van der Waals equation of state by introducing temperature dependency in the values of parameters a and b , as defined in Eq. (1), to provide an overall more accurate model (Redlich and Kwong, 1949). Fig. 1 is a plot of three isotherms obtained from the RK equation of state at sub-critical (94.26°C and 66.85°C) and critical temperature (154.0°C) for R245fa and it is clear that the model deviates considerably at the critical point. Fig. 1 also shows the isotherms in the operating range of the expander and compares them with REFPROP values. The isotherms have better accuracy in this range. The sub-critical isotherms (94.26°C and 66.85°C) are for the inlet and expected outlet temperature of the expander being studied here.

$$p = \frac{R_s T}{v - b} - \frac{a}{\sqrt{T} v (v + b)} \tag{Eq. (1)}$$

$$a = 0.42748 \frac{R_s^2 T_c^{5/2}}{p_c}, b = 0.08662 \frac{R_s T_c}{p_c}$$

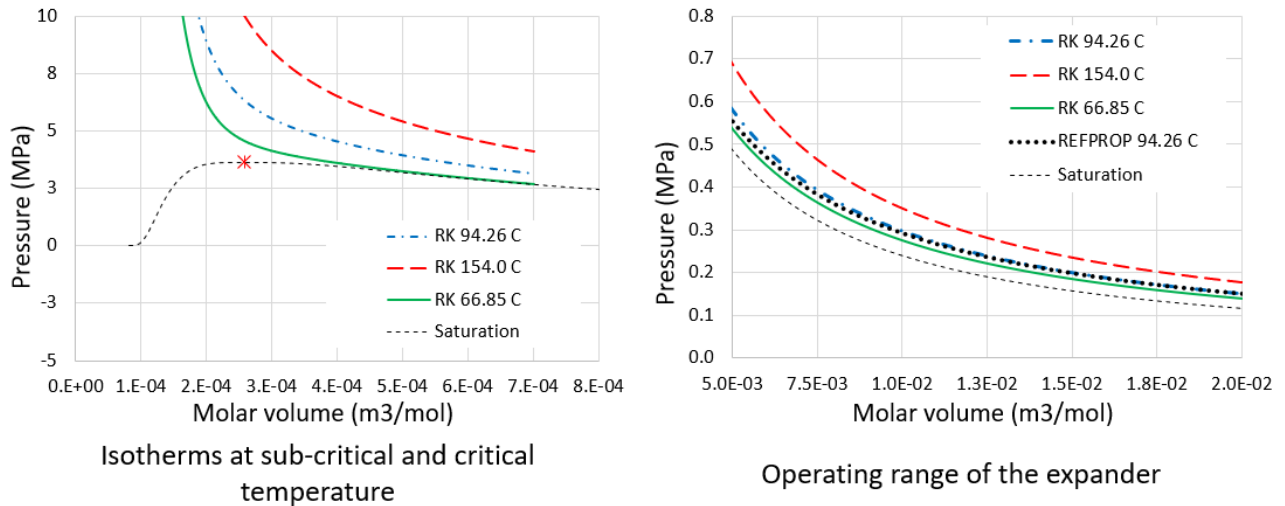


Figure 1: Pressure-volume plots of sub-critical and critical isotherms with RK equation of state and comparison with REFPROP for R245fa

1.2. The Soave Redlich Kwong Equation of State

The SRK equation of state is one of the improved variants of the RK model (Soave, 1972) as defined in Eq. (2). In this model,

the molecular attraction factor is a function of the temperature as well as the fluid acentric factor ω .

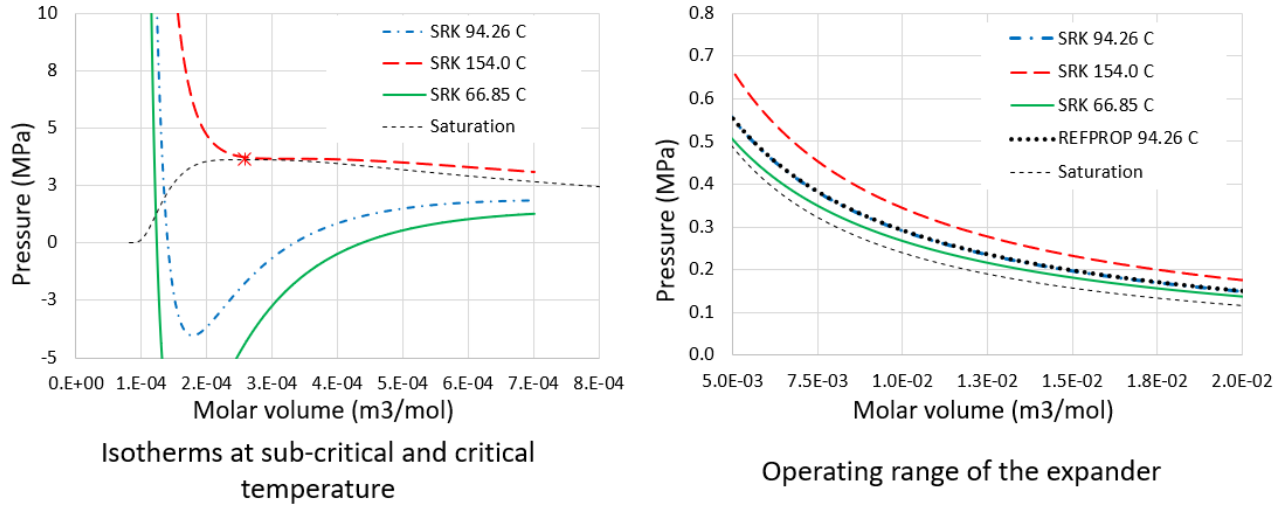


Figure 2: Pressure-volume plots of sub-critical and critical isotherms with SRK equation of state and comparison with REFPROP for R245fa

This version can be applied to fluids with highly asymmetric molecules (Soave, 1972). Fig. 2 is a plot of three isotherms derived with the SRK equation of state at sub-critical and critical temperature for R245fa, from which the improvement in the model close to the critical point can be observed. The isotherms in the operating range of the expander obtained with REFPROP can also be seen in Fig. 2. The isotherms are more accurate in this range than from the RK model. Under sub-critical temperatures, Eq. (2) has three roots for a given pressure. The root with low specific volume corresponds to the liquid phase and the root with the high specific volume corresponds to the vapour phase. The intermediate root of the equation has no physical significance and is not used.

$$p = \frac{R_s T}{v - b} - \frac{\alpha(T) a}{v(v + b)}$$

$$a = 0.42747 \frac{R_s^2 T_c^2}{p_c}, b = 0.08664 \frac{R_s T_c}{p_c} \quad \text{Eq. (2)}$$

$$\alpha(T) = \left(1 + n \left(1 - \sqrt{\frac{T}{T_c}} \right) \right)^2, n = 0.48 + 1.574\omega - 0.176\omega^2$$

1.3. The Aungier Redlich Kwong Equation of State

The ARK model, as defined in Eq. (3), is a further modification of the RK equation, in which the parameters a and b are made to be functions of temperature, the fluid acentric factor ω and the critical specific volume v_c . It is more accurate, especially near to the critical point, as well as for fluids with a negative acentric factor (Aungier, 1995). Isotherm plots of ARK are similar to that of Fig. 2 for R245fa.

$$p = \frac{R_s T}{v - \tilde{b}} - \frac{a(T)}{v^2 + b_0 v}$$

$$a(T) = a_0 \left(\frac{T_c}{T} \right)^n, a_0 = 0.42747 \frac{R_s^2 T_c^2}{p_c}, b_0 = 0.08664 \frac{R_s T_c}{p_c} \quad \text{Eq. (3)}$$

$$c_0 = \frac{R_s T_c}{p_c + \frac{a_0}{v_c^2 + b_0 v_c}} + b_0 - v_c, \tilde{b} = b_0 - c_0, n = 0.4986 + 1.1735\omega + 0.4754\omega^2$$

1.4. The Peng Robinson Equation of State

The PR equation of state model, (Peng and Robinson, 1976), is an improvement over the SRK model and is given in Eq. (4).

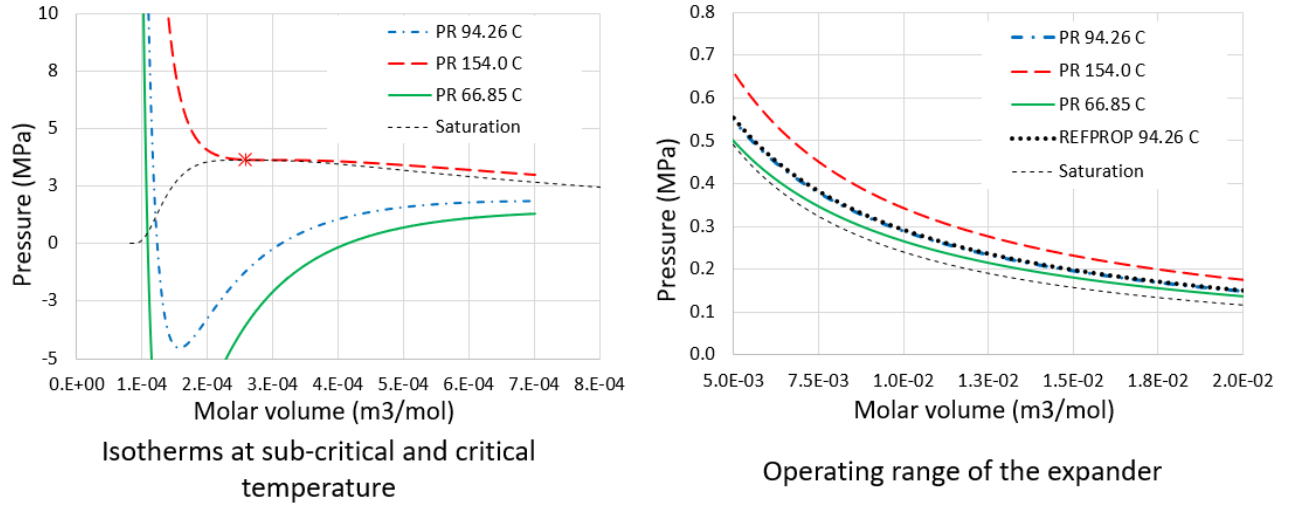


Figure 3: Pressure-volume plots of sub-critical and critical isotherms with PR equation of state and comparison with REFPROP for R245fa

The isotherm plots using it for R245fa are shown in Fig. 3. These are similar to Fig 2 both at sub-critical and critical temperatures and are accurate at the critical point as well as in the expander operating range.

$$p = \frac{R_s T}{v - b} - \frac{\alpha(T) a}{v^2 + 2bv - b^2}$$

$$a = 0.45724 \frac{R_s^2 T_c^2}{p_c}, b = 0.0778 \frac{R_s T_c}{p_c} \quad \text{Eq. (4)}$$

$$\alpha(T) = \left(1 + n \left(1 - \sqrt{\frac{T}{T_c}} \right) \right)^2, n = 0.37464 + 1.54226\omega - 0.26992\omega^2$$

These four equations of state have been used to evaluate the expander performance using a CFD model with R245fa, R290, R1336mzz(Z) and R1233zd(E) as the working fluids, and the results have been compared with those obtained with REFPROP and ideal gas equation.

2. Methodology

The original twin-screw machine was designed as a family of oil flooded air compressors by use of rack generated “N” profiles (Stošić et al. 2005). The range of delivered flows was from 0.6 to 60 m³/min, at delivery pressures of 5 - 13 bar gauge. With a Length/Diameter ratio of 1.55:1 the range of flow was achieved using a set of 5 rotor sizes; 73, 102, 159, 225 and 284 mm main rotor diameter. An end view of the 102 mm rotor pair is shown in Fig. 4 and has been used in the present study as an expander operating with R245fa fluid.

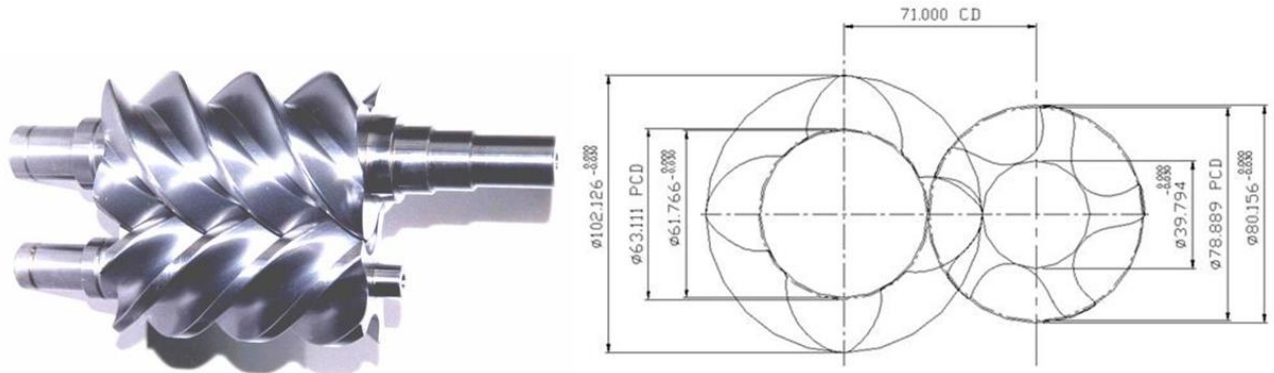


Figure 4: 102 mm Twin-Screw Expander rotors used for the CFD model

The CFD model of the twin-screw expander was based on the use of numerical grids that deform with flow time in order to achieve positive volumetric displacement of the chambers. Kovačević and Rane (2013, 2017) have presented 3D CFD analysis of a dry air twin-screw expander. In this study, the two rotors were each contained in a separate grids and were connected together through non-conformal interfaces. Such interfaces simplify the grid generation procedure but are prone to mass imbalance and leakage over-estimation in the CFD solution (Rane et al., 2013, 2014). Recently, a new grid generation technique has been introduced by the authors which contain both the main and gate rotors in a single grid domain and provide more accurate results (Rane and Kovačević, 2017). These single domain rotor grids are generated by the SCORG tool and have been used here for the CFD model as shown in Fig. 5. For this study, the expander operating condition selected was for a filling pressure of 544 kPa at 94.26°C and a discharge pressure of 175 kPa with a main rotor speed of 3000 rpm.

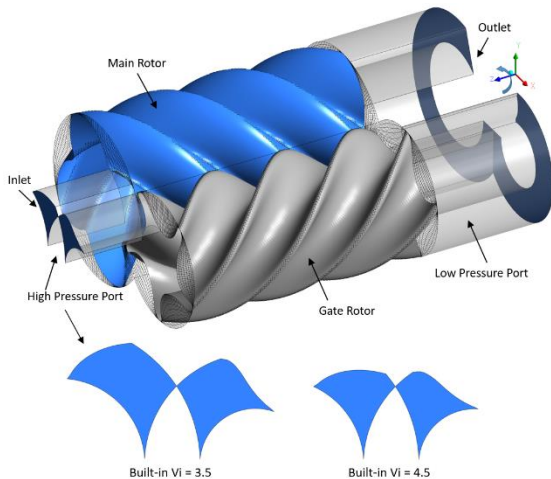


Figure 5: Expander CFD model

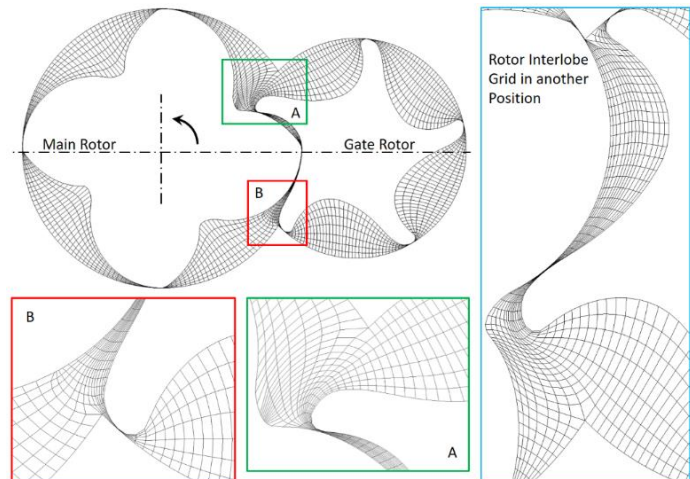


Figure 6: Details in the cross section of the rotor grid

A summary of the expander data for both the main and gate rotors is given in Table 1. It is based on a built-in volume index

(Vi) of 4.5, and the areas of the filling and discharge ports together with the timing of the port opening and closing were calculated taking the wrap angle into consideration.

Table 1. Twin-Screw Expander Details

Profile	N Type	Rotor Data		
Center Distance	71.00 mm		Main Rotor	Gate Rotor
Rotor Length	157.97 mm	Lobes	4	5
Built-in volume Index	4.5	Outer Diameter	101.91 mm	80.17 mm
Interlobe Gap	35 microns	Wrap Angle	306.65°	245.32°
Axial Gap	35 microns	Radial Gap	35 microns	35 microns

The design leakage gaps have been listed in Table 1. In the CFD model both radial and interlobe leakage gaps are accounted by the deforming rotor grid. For simplicity, the axial leakage gaps were not included in the model.

2.1. Rotor Grid Generation

Details of the rotor grid in one of the cross sections are shown in Fig. 6. The entire grid is made of hexahedral cells and the grid quality was optimized for smoothness, expansion factor and orthogonality, by using a partial differential equation based on a quality improvement procedure. Further details of the grid generation can be found in Rane and Kovačević (2017). In this case study, the rotor grid had 200 circumferential nodes on the profile, with 7 radial nodes and 136 axial sections. A summary of the CFD grid size in the rotor and the ports is given in Table 2. In the rotor domain the node coordinates were updated by the solution of the transport equations, as described by Rane and Kovačević (2017). The ports are stationary and get connected to the deforming rotor domain through non-conformal interfaces. The most important grid quality matrices are included in Table 2 and these values are suitable for numerical stability and accuracy for most of the flow solvers in use.

Table 2. CFD grid size and quality metrics

	Nodes	Cells	Orthogonal Angle		Expansion Factor		Aspect Ratio	
			Average	Minimum	Average	Maximum	Average	Maximum
Rotor	431550	380800	64.7	15.1	1.6	632.0	20.9	949.0
LP Port	81918	70400	76.9	34.6	1.1	2.0	2.0	4.0
HP Port	5292	4000	59.1	11.1	1.1	2.0	18.7	45.0

2.2. CFD solver settings

The ANSYS CFX solver was used here for the calculations. The advection scheme was set as first order upwind. Time discretisation was set as fully implicit second order backward Euler and the turbulence model of SST k-Omega with first order discretization was used. The boundary conditions at high pressure inlet were total pressure and temperature, while at the low-pressure outlet it was only static pressure. The main and gate rotors were set as rotating walls with angular speeds of 3000 and 2400 rpm respectively. Since the rotor grid was generated with a 2.2 degrees rotation per step, the solver time step size was set at $1.25e-4$ sec to achieve a main rotor speed of 3000 rpm. The zero pressure, ideal gas specific heat c_p^0 , required for the calculation of internal energy and entropy, was derived from a 4th order polynomial. The critical state temperature and pressure for R245fa were input to generate a lookup table in the 250 and 400 K temperature range, while the pressure range was between 25 and 6000 kPa. The input values for the c_p^0 polynomial, the critical point properties, the acentric factor and the molar mass were all taken from REFPROP and Eq. (5) was obtained using them with the reference state values taken as 101.325 kPa, and 25°C. Fluid specific properties for R245fa were $\omega = 0.3776$, boiling temperature = 288.29 K, $p_c = 36.51$ bar, $T_c = 427.16$ K, $v_c = 259.7466$ cm³ mol⁻¹ and molar mass = 134.05 kg kmol⁻¹.

$$\frac{c_p^0}{R_s} = c_0 T^0 + c_1 T^1 + c_2 T^2 + c_3 T^3 + c_4 T^4 \quad \text{Eq. (5)}$$

$$c_0 = 6.39, c_1 = -0.0012577, c_2 = 0.00019441, c_3 = -4.7081e - 07, c_4 = 3.8563e - 10,$$

Dynamic viscosity and thermal conductivity were specified using the kinetic theory model and critical volume v_c as an input (Chung et al, 1988). In Eq (6), μ is the dynamic viscosity in μP , M is the molecular weight in g mol^{-1} , σ is the collision diameter in Angstroms and $\Omega(T) = 1.0$ for a rigid, non-interacting sphere model.

$$\mu = 26.69 \frac{\sqrt{MT}}{\Omega(T)\sigma^2} \quad \text{Eq. (6)}$$

$$\sigma = 0.809^3 \sqrt{v_c}$$

The modified Eucken thermal conductivity model described in Poling et al. (2001) was used and is formulated in Eq (7). Here, λ is the thermal conductivity, R_s is the specific gas constant.

$$\frac{\lambda}{\mu c_v} = 1.32 + \frac{1.77 R_s}{c_v} \quad \text{Eq. (7)}$$

Each case was solved for four revolutions of the main rotor such that pressure, temperature and mass flow rate through the boundaries showed a cyclic repetition. Cycle averaged data from last four cycles was used for expander performance evaluation.

In the CFD solution, both the thermodynamic properties and the transport properties of the fluid contribute to the accuracy of estimation of performance of the expander. In figures 1 to 3, the specific volumes were compared over the operating range of the expander. In order to compliment these plots, a comparison of specific volume obtained from each of the real gas equation of state and REFPROP has been reported in Table 3. For REFPROP fluid setup, once the data is provided to the solver in the form of a real gas property file, the solver internally allocates specific volume and specific heat property from this data. In case of the real gas equation of state, specific volume is specified through solution of Eq. (1 to 4) and specific heat is defined by Eq. (5). In case of the ideal gas equation of state, specific heat is defined by Eq. (8). Three operating pressures and temperature conditions used here correspond to the expander's filling state, intermediate state and the delivery condition at the exit. RK equation of state deviates from REFPROP in the range of 1 – 1.5%. Both ARK and SRK equations for state deviate to a smaller extent in the order of 0.5%. PR equation deviates by a very small fraction of the order of 0.2% from REFPROP. Ideal gas equation of state deviates considerably in the range of 4 – 11%. Deviation in specific heat is of the order of 3 – 6% for the real gas equations of state and REFPROP. But in case of the ideal gas, the deviation is higher in the order of 16 – 22%. This high difference is due to the difference in the polynomial used. For real gas equations, zero pressure coefficients are supplied to the solver which integrates internal energy and entropy based on Eq. (5). Whereas, in case of ideal gas, this integration option is not available and a second order polynomial as a function of temperature was used whose coefficients are obtained from REFPROP at saturation over the temperature range 20.0°C to 100.0°C. The polynomial coefficients for R245fa are in Eq. (8) and temperature is in K units.

$$c_p = c_0 T^0 + c_1 T^1 + c_2 T^2 \quad \text{Eq. (8)}$$

$$c_0 = 1610.20, c_1 = -8.5679, c_2 = 0.0212$$

Table 3. Comparison of thermodynamic and transport properties for R245fa

R254fa	Specific Volume		Specific Heat		Thermal Conductivity		Dynamic Viscosity	
	(kg m ⁻³)	(%)	(J kg ⁻¹ K ⁻¹)	(%)	(W m ⁻¹ K ⁻¹)	(%)	(Pa s)	(%)
NIST-REFPROP								
544 kPa, 94.26°C	0.0378593		1081.82		0.0309538		2.22309E-05	
360 kPa, 80.00°C	0.0563997		1036.13		0.0294081		2.17952E-05	
175 kPa, 65.00°C	0.1149240		977.24		0.0275851		2.13273E-05	
Redlich Kwong								
544 kPa, 94.26°C	0.0384156	1.5	1009.99	6.6	0.0294655	4.8	2.22311E-05	0.001
360 kPa, 80.00°C	0.0571779	1.4	977.16	5.7	0.0281851	4.2	2.17953E-05	0.000
175 kPa, 65.00°C	0.1159760	0.9	941.68	3.6	0.0268441	2.7	2.13275E-05	0.001
Soave Redlich Kwong								
544 kPa, 94.26°C	0.0380734	0.6	1020.70	5.6	0.0294655	4.8	2.22311E-05	0.001
360 kPa, 80.00°C	0.0567543	0.6	983.90	5.0	0.0281849	4.2	2.17954E-05	0.001
175 kPa, 65.00°C	0.1154710	0.5	944.81	3.3	0.0268441	2.7	2.13275E-05	0.001
Aungier Redlich Kwong								
544 kPa, 94.26°C	0.0380414	0.5	1030.87	4.7	0.0294655	4.8	2.22311E-05	0.001
360 kPa, 80.00°C	0.0566969	0.5	991.95	4.3	0.0281849	4.2	2.17954E-05	0.001
175 kPa, 65.00°C	0.1153770	0.4	949.44	2.8	0.0268441	2.7	2.13275E-05	0.001
Peng Robinson								
544 kPa, 94.26°C	0.0378021	0.2	1019.77	5.7	0.0294655	4.8	2.22311E-05	0.001
360 kPa, 80.00°C	0.0564841	0.1	983.21	5.1	0.0281849	4.2	2.17954E-05	0.001
175 kPa, 65.00°C	0.1152030	0.2	944.44	3.4	0.0268441	2.7	2.13275E-05	0.001
Ideal Gas								
544 kPa, 94.26°C	0.0418916	10.7	1324.06	22.4	0.0394747	27.5	2.22309E-05	0.000
360 kPa, 80.00°C	0.0608459	7.9	1228.40	18.6	0.0359491	22.2	2.17952E-05	0.000
175 kPa, 65.00°C	0.1198520	4.3	1137.09	16.4	0.0326066	18.2	2.13273E-05	0.000

Thus, for the ideal gas, an overall higher specific heat will reflect in the CFD solution as a higher local temperature. Transport properties include the thermal conductivity and dynamic viscosity and have been compared in Table 3. For consistency, transport properties of REFPROP fluid as well as all real gas and the ideal gas equation of state fluids were specified using kinetic theory model defined by Eq. (6) and (7). Accordingly, Table 3 validates these properties where the thermal conductivity is within 5% for the real gas equations and dynamic viscosity is identical. In case of ideal gas, the thermal conductivity variation is higher due to the higher difference of specific heat.

2.3. Extended analysis with low GWP alternatives

An extended analysis was carried out with R245fa, varying the expander's built-in volume index and operating speed. With a change in V_i , the internal pressure, temperature and specific properties of the fluid will have different variation during the expansion process. Three alternative, low GWP working fluids to R245fa; R290 was evaluated at operating pressure of 600 kPa and temperature of 130.0°C, while R1336mzz(Z) and R1233zd(E) were both evaluated at operating pressure of 600 kPa and temperature of 110.0°C during the induction to the expander. Results from the extended analysis included additional 30 test cases with all the real gas equations of state and REFPROP data. A comparison of the expander performance and CPU time requirements has been presented in each of the operating condition to evaluate the accuracy and computational time saving obtained with the real gas definition for these fluids.

3. Results and Discussion

The expander CFD model was evaluated with six specifications of R245fa properties as listed in Table 3. Results showing the comparison between the fluid models are presented here in terms of the expander performance, internal pressure variation during the expansion cycle, local distribution of pressure, temperature and specific volume. Also, some of the computational metrics have been reported in order to compare the CFD calculation effort.

3.1. Performance prediction

Table 4 summarises the expander performance as predicted by the CFD model when using the selected alternative procedures for calculating the properties of fluid R245fa. The first case (1) was obtained from REFPROP. The other four cases (2 – 5) were obtained using a real gas cubic equation of state as described in Section 1 and which are directly available in the solver for selection as the fluid model. The last case (6) was obtained using an ideal gas equation of state for the purpose of comparison.

Table 4. R245fa fluid specification in expander's CFD model and comparison of performance data

Case	R254fa fluid Data	Flow		Power		Specific Power		e_p	
		(kg s ⁻¹)	(%)	(kW)	(%)	(kW kg ⁻¹ s)	(kW kg ⁻¹ s)	(%)	
1	NIST REFPROP	0.25939		3.114		12.006			
2	Redlich Kwong	0.25677	1.01	3.091	0.74	12.038	0.15	1.27	
3	Soave Redlich Kwong	0.25870	0.26	3.100	0.47	11.982	0.06	0.54	
4	Aungier Redlich Kwong	0.25890	0.19	3.099	0.48	11.971	0.06	0.52	
5	Peng Robinson	0.26012	-0.28	3.115	-0.04	11.977	0.03	0.28	
6	Ideal Gas	0.23904	7.84	2.968	4.69	12.417	1.22	10.17	

REFPROP solution has been used here as references \dot{m}_r for mass flow rate and P_r for indicated power. Error e_p in the specific power P_s were calculated using Eq (9).

$$e_p = \sqrt{\left(\frac{\partial P_s}{\partial \dot{m}} \delta \dot{m}\right)^2 + \left(\frac{\partial P_s}{\partial p} \delta p\right)^2} \quad \text{Eq. (9)}$$

$$P_s = \frac{P}{\dot{m}}, \delta \dot{m} = \dot{m}_r - \dot{m}, \delta P = P_r - P, \% \text{ error} = \frac{e_p}{P_r} 100\%$$

It can be observed from Table 4 that, of the real gas models, RK equation of state has the highest deviation in estimation of flow, power and specific power, although it is within 1.3%. Whereas, the PR equation of state is in close agreement with REFPROP with deviation of the order of 0.3%, which for practical purposes, is negligible. Both the SRK and ARK equations of state produce flow, power and specific power with a deviation of less than 0.6% with respect to REFPROP. These can all, therefore, be considered as accurate enough to be used in the selected operating condition of the expander. However, results using the ideal gas equation of state deviate significantly from those obtained from REFPROP with differences in flow of 7.84%, indicated power of 4.69% and specific power exceeding 10%. Hence, an ideal gas equation should not be used under these operating conditions using R245fa.

3.2. Pressure distribution

Geometrical characteristics of the expander such as chamber volume variation, high pressure filling area and low pressure discharge area variation with the main rotor angle are presented in Fig. 7. The expander filling pressure was 544 kPa and the discharge pressure was 175 kPa. Fig. 7 also shows the pressure distribution during the filling, expansion and discharge processes.

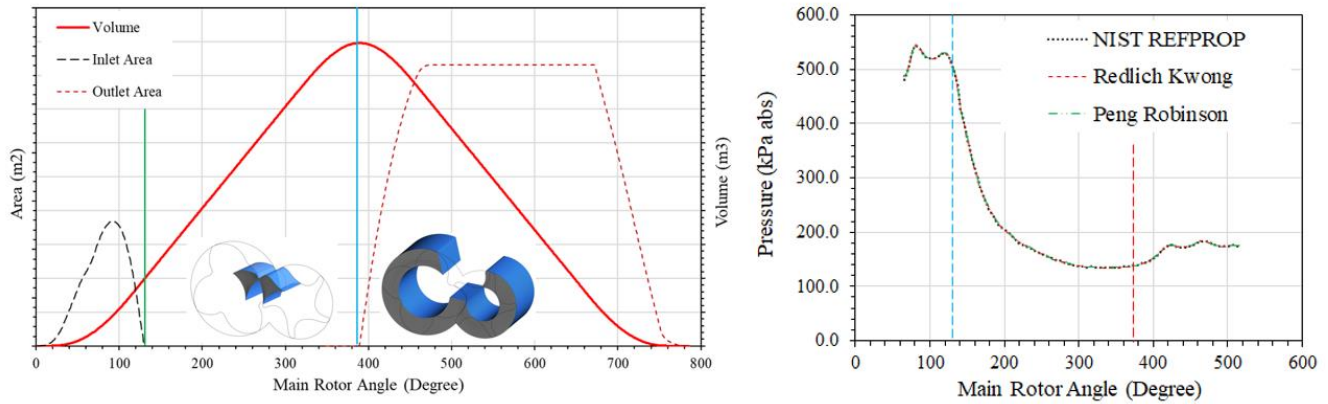


Figure 7: Geometrical characteristics of the expander and comparison of internal pressure during expansion

As observed from Fig. 7, the use of REFPROP and the RK and PR equations of state models, result in identical pressure variation with main rotor angle. For clarity, the pressure distribution using SRK and ARK, not plotted here, but also overlapped with these results and indicate that in the operating conditions of the expander these real gas equations of state can be used with good accuracy. The distribution of instantaneous pressure on the rotor surfaces and in the ports is shown in Fig. 8, when using REFPROP. The pressure ranges from 100 to 544 kPa. Comparing these results with Fig. 7, it is confirmed that assuming a built-in volume index of 4.5, results in over expansion in the working chambers, before discharge begins. Within each of the screw chambers, pressure distribution is uniform.

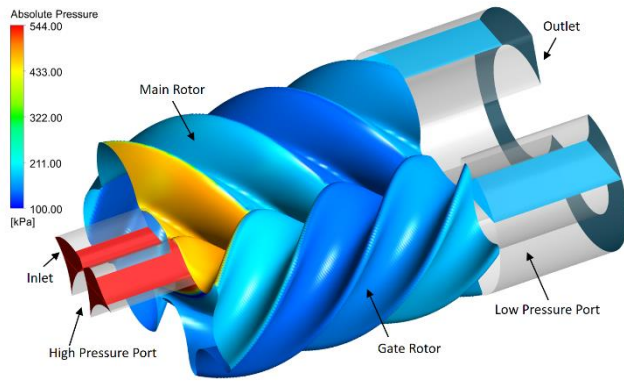


Figure 8: Instantaneous pressure distribution

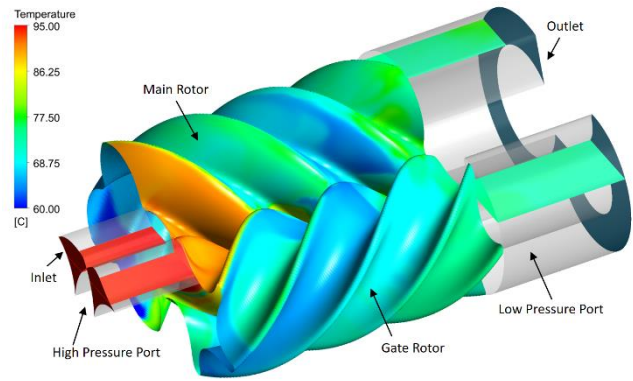


Figure 9: Instantaneous temperature distribution

3.3. Temperature distribution

The distribution of instantaneous temperature on the rotor surfaces and in the ports is shown in Fig. 9 when using REFPROP. The temperature ranges from 60 to 95°C and within the screw chambers, a local variation is visible. This is due to the interaction of the gas volume in the chamber with leakage gas streams and the rotor dynamics.

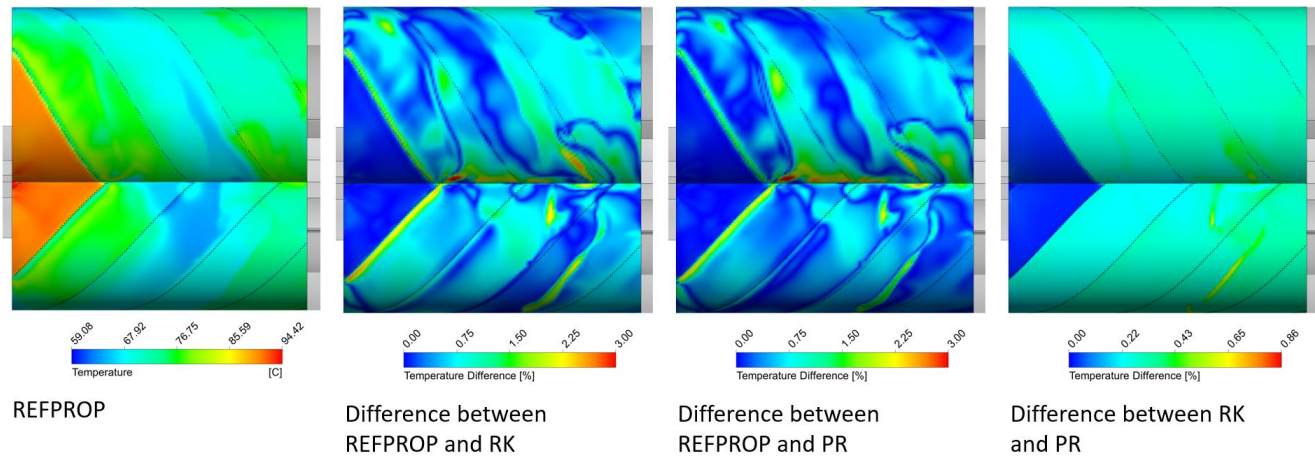


Figure 10: Comparison of local temperature distribution

When using REFPROP to calculate the distribution of instantaneous temperature on the rotor housing, the results are shown in Fig. 10. This is in the same range as that on the rotor surfaces shown in Fig. 9, but when using the RK and PR equation of state the differences from the REFPROP results are shown in Figs. 10. In both the RK and PR models, the maximum temperature deviation is less than 3%, the same order of deviation was obtained using the SRK and ARK models. The difference in instantaneous temperature between the results from the RK and PR equation of state models, shown in Fig. 10 is less than 0.86%. All the four equation of state models considered here are thus suitable for the operating condition of the expander.

3.4. Specific Volume variation

The distribution of instantaneous specific volume on the rotor housing surfaces is shown in Fig. 11, when using REFPROP, also the differences in instantaneous specific volume on the rotor housing using the RK and PR equations compared with REFPROP is shown in Fig. 11. The RK model has a maximum deviation of 17.53% in a few local cells present in the leakage gaps while it is slightly lower in case of PR model at 15.59% in similar local leakage regions.

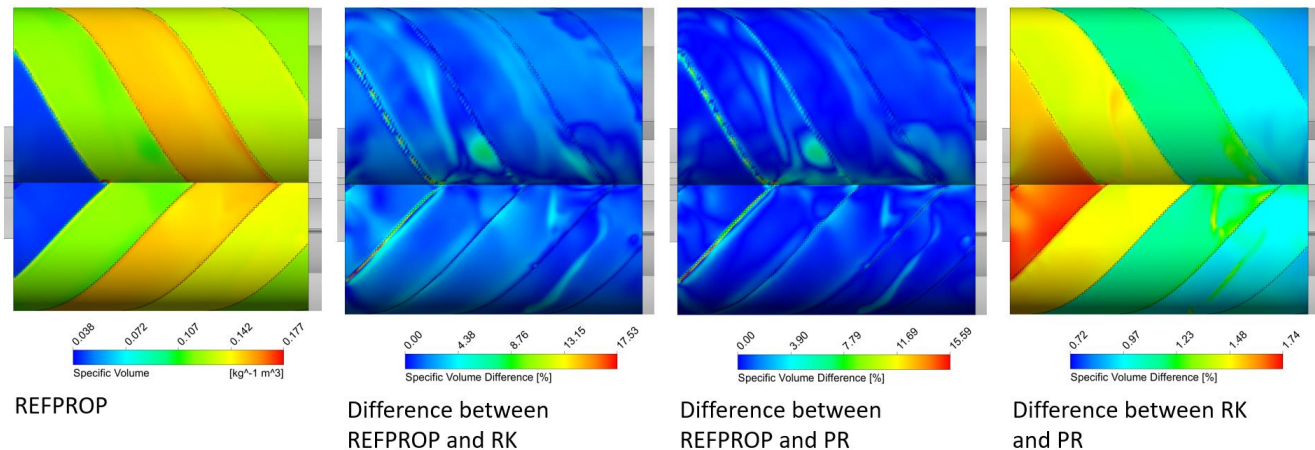


Figure 11: Comparison of local specific volume distribution

The specific volume deviation with the SRK and ARK models, was of the same order, while the difference in instantaneous specific volume between the RK and PR equations is shown in Fig. 11. There, the maximum deviation is 1.74%. On average, the deviation in specific volume is less than 5% and all four equation of state models considered here are accurate enough

under the given operating conditions. A comparison of mass flow rate in Table 4 indicates that these local deviations in specific volume result in a very small difference in the cycle averaged mass flow rate through the expander.

3.5. Computational metrics comparison

A summary of some of the computational metrics related to the CFD calculations is given in Table 5. Case 1a is with REFPROP fluid data. It has same number of solver iterations (equal to 5 per time step) as that of cases 2 – 5 which are with the real gas equation of state models. Case 1b is also with REFPROP fluid data, but here the number of solver iterations have been increased to 8 per time step in order to reach the same level of numerical convergence as that obtained with the real gas cases 2 – 5.

Table 5. Comparison of computational metrics for the various fluid models

Case	R254fa fluid Data	Solver iterations	Normalized convergence level				CPU cores	CPU time (hr rev ⁻¹)
			Continuity	Energy	Momentum-w	average		
1a	NIST-REFPROP	5	1.53	2.16	1.64	1.78	6	3.95
1b	NIST-REFPROP	8	1.00	1.00	1.00	1.00	6	6.21
2	Redlich Kwong	5	0.81	1.16	1.13	1.03	6	3.88
3	Soave Redlich Kwong	5	0.81	1.14	1.13	1.02	6	3.79
4	Aungier Redlich Kwong	5	0.81	1.14	1.13	1.02	6	3.79
5	Peng Robinson	5	0.81	1.14	1.13	1.02	6	3.95
6	Ideal Gas	5	0.81	1.14	1.13	1.02	6	3.97

At the end of a time step, Case 1b residual levels were found to be $5.80E^{-05}$ for continuity, $5.10E^{-04}$ for energy and $5.60E^{-04}$ for momentum. These values have been used in Table 5 for normalization so that the difference in order of magnitude is apparent for Case 1a. A mass imbalance was calculated between the cyclically averaged mass flow rate at the inlet and outlet of the expander and a high level of conservation (within 0.5%) was obtained with all the cases. The recorded CPU time in Table 5 indicates that Case 1b with the higher number of solver iterations, required 57% higher calculation time to reach to the same order of numerical convergence as that in Cases 2 – 5. Case 6 obtained with the ideal gas equation of state also took the same computational time as any of the real gas models.

3.6. R245fa at 1500 rpm, built-in volume index of 4.5

When the expander is operated at a lower speed, the influence of leakage is higher on the flow and thus the specific power output can drop. In terms of the numerical setup, most of the factors remain identical to that described in section 1. However, the main and gate rotors were set as rotating walls with angular speeds of 1500 and 1200 rpm respectively. Since the rotor grid was generated with a 2.2 degrees rotation per step, the solver time step size was set at $2.5e^{-4}$ sec to achieve a main rotor speed of 1500 rpm. Table 6 summarises the expander performance as predicted by the CFD model when using the real gas equation of state, ideal gas and REFPROP data for R245fa. Similar to the results presented in Table 4, here, the first case (1) was obtained from REFPROP. The other four cases (2 – 5) were obtained using a real gas cubic equation of state as described in Section 1 and the last case (6) was obtained using an ideal gas equation of state for the purpose of comparison. The specific power of the expander has dropped from $12.0 \text{ kW kg}^{-1} \text{ s}$ at 3000 rpm to $9.973 \text{ kW kg}^{-1} \text{ s}$ at 1500 rpm. It can be observed from Table 6 that, of the real gas models, PR equation of state has the highest deviation in estimation of flow and specific power, although it is within 0.8%. Whereas, the RK, SRK and ARK equation of state are in close agreement with REFPROP with deviation of the order of 0.4%. Deviations of the order of 1-2 % are negligible for practical purposes. The real gas equations can all, therefore, be considered as accurate enough to be used in the selected operating condition of the expander. However, results using the ideal gas equation of state deviate significantly from those obtained from REFPROP with differences in flow of 6.43%, indicated power of 2.14% and specific power exceeding 7.5%. The recorded CPU time in Table 6 indicates that Case 1 with the REFPROP, required 57% higher calculation time to reach to the same order of numerical convergence as that

in Cases 2 – 5. Case 6 obtained with the ideal gas equation of state also took the same computational time as any of the real gas models.

Table 6. R245fa performance data at 1500 rpm, built-in $V_i = 4.5$, Inlet Pressure = 544 kPa and Temperature = 94.26°C

Case	R254fa fluid Data	Flow		Power		Specific Power		CPU Time	
		(kg s ⁻¹)	(%)	(kW)	(%)	(kW kg ⁻¹ s)	(%)	(hr rev ⁻¹)	(%)
1	NIST REFPROP	0.17686		1.764		9.973		5.85	57.05
2	Redlich Kwong	0.17635	0.29	1.760	0.24	9.978	0.38	3.72	-0.11
3	Soave Redlich Kwong	0.17746	-0.34	1.762	0.12	9.927	0.36	3.71	-0.45
4	Aungier Redlich Kwong	0.17757	-0.40	1.761	0.14	9.920	0.42	3.73	0
5	Peng Robinson	0.17827	-0.79	1.766	-0.15	9.909	0.80	3.73	0
6	Ideal Gas	0.16549	6.43	1.726	2.14	10.431	7.54	3.70	-0.67

3.7. R245fa at 3000 rpm, built-in volume index of 3.5

The chamber volume variation with main rotor rotation angle is presented in Fig. 7. From this plot, it can be seen that the filling port closes at around 115° and the chamber volume expands to a maximum at about 395° rotor angle. The ratio of these two volumes dictates the internal built-in volume index V_i of the expander. Fig 7. Inlet area is for a $V_i = 4.5$. When V_i is reduced to 3.5 the port remains open for further 25° and the filling area is larger in the CFD model as shown in Fig. 5. A difference in V_i produces difference in flow and indicated power output from the expander, even though it is running at the same pressure and temperature and at same rotor speed. Due to a V_i of 3.5, the specific power of the expander has increased from 12.0 kW kg⁻¹ s at a V_i of 4.5 to 14.232 kW kg⁻¹ s. Table 7 summarises the expander performance as predicted by the CFD model when using the selected alternative procedures for calculating the properties of fluid R245fa. It can be observed from Table 7 that, of the real gas models, RK equation of state has the highest deviation in estimation of flow, power and specific power, although it is within 0.8%. Both the SRK and ARK equations of state produce flow, power and specific power with a deviation of less than 0.2% with respect to REFPROP. The PR equation of state is also in close agreement with REFPROP with deviation of the order of 0.53%. These can all, therefore, be considered as accurate enough to be used in the selected operating condition of the expander. However, again results using the ideal gas equation of state deviate significantly from those obtained from REFPROP with differences in flow of 7.16%, indicated power of 2.89% and specific power exceeding 8.5%.

Table 7. R245fa performance data at 3000 rpm, built-in $V_i = 3.5$, Inlet Pressure = 544 kPa and Temperature = 94.26°C

Case	R254fa fluid Data	Flow		Power		Specific Power		CPU Time	
		(kg s ⁻¹)	(%)	(kW)	(%)	(kW kg ⁻¹ s)	(%)	(hr rev ⁻¹)	(%)
1	NIST REFPROP	0.33523		4.771		14.232		5.758	52.88
2	Redlich Kwong	0.33285	0.71	4.753	0.38	14.279	0.81	3.771	0.11
3	Soave Redlich Kwong	0.33521	0.00	4.761	0.21	14.203	0.21	3.767	0.00
4	Aungier Redlich Kwong	0.33545	-0.06	4.761	0.21	14.192	0.22	3.771	0.11
5	Peng Robinson	0.33700	-0.53	4.775	-0.10	14.170	0.53	3.767	0.00
6	Ideal Gas	0.31122	7.16	4.633	2.89	14.887	8.65	3.658	-2.88

The recorded CPU time in Table 7 indicates that REFPROP definition required 53% higher calculation time to reach to the same order of numerical convergence as that in Cases 2 – 5. The ideal gas equation of state took approximately 3% lower computational time than any of the real gas models.

3.8. R290 at 3000 rpm, built-in volume index of 4.5

In order to increase the validity of the results presented here to a wider range, another light hydrocarbon R290 has been tested on the same expander but under different operating pressure and temperature. In this case the filling pressure was set at 600 kPa and temperature of 130.0 °C. With a low GWP of 3.3, R290 has favourable thermodynamic properties such as higher critical pressure, but its use has been limited due to an auto-ignition temperature of 494°C and flammability. The fluid has a safety group rating - A3 in ASHRAE Standard 34, 2010. The CFD case setup remains identical to that used for the R245fa cases and only the new fluid is introduced with its own specific thermodynamic and transport properties. The definition of real gas equation of state follows Eq. (1) to (4) for evaluation of specific volume. In case of R290, the zero pressure, ideal gas specific heat c_p^0 , required for the calculation of internal energy and entropy, was also derived from a 4th order polynomial. The critical state temperature and pressure were input to generate a lookup table in the temperature range of 200 and 460 K, while the pressure was set in the range of 25 and 4000 kPa. The input values for the c_p^0 polynomial, the critical point properties, the acentric factor and the molar mass were all taken from REFPROP and Eq. (10) was obtained using them with the reference state values taken as 101.325 kPa, and 25°C. Fluid specific properties for R290 were $\omega = 0.1521$, boiling temperature = 231.036 K, $p_c = 42.512 \text{ bar}$, $T_c = 369.89 \text{ K}$, $v_c = 200.00 \text{ cm}^3 \text{ mol}^{-1}$ and molar mass = 44.09562 kg kmol⁻¹.

$$\frac{c_p^0}{R_s} = c_0 T^0 + c_1 T^1 + c_2 T^2 + c_3 T^3 + c_4 T^4 \quad \text{Eq. (10)}$$

$$c_0 = 8.28793412613593, c_1 = -4.14176186389276e^{-2}, c_2 = 2.38806313319961e^{-4}, c_3 = -3.7933471834826e^{-7}, c_4 = 2.17029933333171e^{-10},$$

Similar to R245fa, dynamic viscosity and thermal conductivity were specified using the kinetic theory model and critical volume v_c as an input in Eq. (6) and Eq. (7) respectively. For the ideal gas equation of state, a third order polynomial as a function of temperature was used for specific heat whose coefficients are obtained from REFPROP at saturation over the temperature range 0.0°C to 150.0°C. The polynomial coefficients for R290 are in Eq. (11) and temperature is in K units.

$$c_p = c_0 T^0 + c_1 T^1 + c_2 T^2 + c_3 T^3 \quad \text{Eq. (11)}$$

$$c_0 = 921.614, c_1 = -4.77411e^{-1}, c_2 = 1.38396e^{-2}, c_3 = -1.29939e^{-5}$$

Due to the higher filling pressure used for R290, it is expected that the power output from the expander will increase thereby increasing the specific power output. Moreover, R290 with a lower molecular weight will have lower density. Hence for the expander's fixed volumetric displacement, the mass flow rate of R290 will be considerably lower than that with R245fa thus further increasing the specific power output.

Table 8. R290 performance data at 3000 rpm, built-in Vi = 4.5, Inlet Pressure = 600 kPa and Temperature = 130.0°C

Case	R290 fluid Data	Flow (kg s ⁻¹)	(%)	Power (kW)	(%)	Specific Power (kW kg ⁻¹ s)	(%)	CPU Time (hr rev ⁻¹)	(%)
1	NIST REFPROP	0.10802	0	4.13376	0	38.267	0	6.09	54.77
2	Redlich Kwong	0.10844	-0.38	4.13645	-0.06	38.146	0.383	3.90	-0.95
3	Soave Redlich Kwong	0.10783	0.18	4.13377	0.00	38.334	0.18	3.93	0.00
4	Aungier Redlich Kwong	0.10785	0.16	4.13520	0.03	38.343	0.17	3.90	-0.95
5	Peng Robinson	0.10873	-0.65	4.13943	-0.13	38.070	0.66	3.93	0.00
6	Ideal Gas	0.10510	2.71	4.09596	0.91	38.971	2.98	3.85	-2.22

Table 8 summarises the expander performance as predicted by the CFD model. Under these operating conditions and with R290 fluid, the power output is higher at 4.13376 kW with R290 as compared to 3.114 kW with R245fa. The mass flow rate

of R290 is only 0.10802 kg s⁻¹ as compared to 0.25939 kg s⁻¹ with R245fa. Hence, the specific power output from the expander is nearly three times higher at 38.267 kW kg⁻¹ s as compared to the R245fa at 12.006 kW kg⁻¹ s. It can be observed from Table 8 that, of the real gas models, PR equation of state has the highest deviation in estimation of flow (0.65%), power (0.13%) and specific power is close to 0.66%, practically very small. The RK equation of state produces flow, power and specific power with a deviation of less than 0.38% and both the SRK and ARK equations of state show a deviation of less than 0.2% with respect to REFPROP. These can all, therefore, be considered as accurate enough to be used in the selected operating condition of the expander even for the fluid R290. Results using the ideal gas equation of state deviate from REFPROP with differences in flow of 2.71%, indicated power of 0.91% and specific power about 1.14%. Due to lower molar mass, deviations for R290 are not as significant as with R245fa. The recorded CPU time in Table 8 indicates that REFPROP required 55% higher calculation time to reach to the same order of numerical convergence as that in Cases 2 – 5. Case 6, with the ideal gas equation of state took about 2.22% lower computational time than any of the real gas models.

3.9. R1336mzz(Z) at 3000 rpm, built-in volume index of 4.5

An Organic Rankine Cycle performance comparison with R245fa and low GWP alternative working fluids R1233zd(E) and R1336mzz(Z) has been reported in Molés et al. (2014) over a range of evaporating and condensing temperatures and vapour superheats. The low GWP alternatives with favourable thermodynamic properties such as lower vapour pressure and higher critical temperature resulted in lower pumping power and higher net cycle efficiencies. In comparison to R245fa, R1233zd(E) could enable about 10.6% and R1336mzz(Z) about 17% higher net cycle efficiency, respectively. R1336mzz(Z) has a GWP of 2 and a high safety group rating - A1 in ASHRAE Standard 34, 2010 (Lemmon et al., 2018). Here, the R1336mzz(Z) expander was calculated with 3000 rpm operating speed at 600 kPa pressure and 110.0 °C temperature. The new fluid is introduced in the CFD model with its own specific thermodynamic and transport properties. The definition of real gas equation of state follows Eq. (1) to (4) for evaluation of specific volume. In case of R1336mzz(Z), the zero pressure, ideal gas specific heat c_p^0 , required for the calculation of internal energy and entropy, was also derived from a 4th order polynomial. The critical state temperature and pressure were input to generate a lookup table in the temperature range of 180 and 400 K, while the pressure was set in the range of 25 and 2500 kPa. The input values for the c_p^0 polynomial, the critical point properties, the acentric factor and the molar mass were all taken from REFPROP and Eq. (12) was obtained using them with the reference state values taken as 101.325 kPa, and 25°C. Fluid specific properties for R1336mzz(Z) were $\omega = 0.386$, boiling temperature = 306.603 K, $p_c = 29.03 \text{ bar}$, $T_c = 444.5 \text{ K}$, $v_c = 328.515 \text{ cm}^3 \text{ mol}^{-1}$ and molar mass = 164.056 kg kmol⁻¹.

$$\frac{c_p^0}{R_s} = c_0 T^0 + c_1 T^1 + c_2 T^2 + c_3 T^3 + c_4 T^4 \quad \text{Eq. (12)}$$

$$c_0 = -10.948110963, c_1 = 1.6239808023e^{-1}, c_2 = -3.0152212094e^{-4}, c_3 = 2.3029629584e^{-7}, c_4 = -2.3466067698e^{-11},$$

Similar to R245fa, dynamic viscosity and thermal conductivity were specified using the kinetic theory model and critical volume v_c as an input in Eq. (6) and Eq. (7) respectively. For the ideal gas equation of state, a fourth order polynomial as a function of temperature was used for specific heat whose coefficients are obtained from REFPROP at saturation over the temperature range -45.0°C to 130.0°C. The polynomial coefficients for R1336mzz(Z) are in Eq. (13) and temperature is in K units.

$$c_p = c_0 T^0 + c_1 T^1 + c_2 T^2 + c_3 T^3 + c_4 T^4 \quad \text{Eq. (13)}$$

$$c_0 = 7.7658272967e^3, c_1 = -1.070144921e^2, c_2 = 5.8022981565e^{-1}, c_3 = -1.354021251e^{-3}, c_4 = 1.1793033724e^{-6}$$

Due to the higher filling pressure used for R1336mzz(Z), it is expected that the flow and power output from the expander will increase thereby increasing the specific power output. Table 9 summarises the expander performance as predicted by the CFD model. The power output is higher at 4.06612 kW with R1336mzz(Z) as compared to 3.114 kW with R245fa. However, the

specific power of the expander has not changed much from 12.006 kW kg⁻¹ s with R245fa and is relatively lower at 11.972 kW kg⁻¹ s with R1336mzz(Z). This can be due to the much higher density of R1336mzz(Z) that increases the mass flow rate to 0.33964 kg s⁻¹ as compared to 0.25939 kg s⁻¹ with R245fa. It can be observed from Table 9 that, of the real gas models, RK equation of state has the highest deviation in estimation of flow, power and specific power, although it is within 2.2%. Whereas, the PR equation of state is in close agreement with REFPROP with deviation of the order of 0.3%, which for practical purposes, is negligible. Both the SRK and ARK equations of state produce flow, power and specific power with a deviation of about 1.1% with respect to REFPROP, which is again negligible. These can all, therefore, be considered as accurate enough to be used in the selected operating condition of the expander with R1336mzz(Z). Results using the ideal gas equation of state again deviate significantly from those obtained from REFPROP with differences in flow of 10.6%, indicated power of 6.58% and specific power exceeding 14.41%.

Table 9. R1336mzz(Z) performance data at 3000 rpm, built-in $V_i = 4.5$, Inlet Pressure = 600 kPa and Temperature = 110.0°C

Case	R1336mzz(Z) fluid Data	Flow		Power		Specific Power		CPU Time	
		(kg s ⁻¹)	(%)	(kW)	(%)	(kW kg ⁻¹ s)	(%)	(hr rev ⁻¹)	(%)
1	NIST REFPROP	0.33964	0	4.06612	0	11.972	0	5.96	55.54
2	Redlich Kwong	0.33323	1.89	4.02490	1.01	12.078	2.20	4.01	4.67
3	Soave Redlich Kwong	0.33664	0.88	4.04014	0.64	12.001	1.10	3.84	0.11
4	Aungier Redlich Kwong	0.33701	0.77	4.04036	0.63	11.989	1.01	4.01	4.67
5	Peng Robinson	0.33891	0.21	4.05756	0.21	11.972	0.30	3.83	0.00
6	Ideal Gas	0.30364	10.60	3.79876	6.58	12.511	14.41	3.75	-2.28

The recorded CPU time in Table 9 indicates that REFPROP required 56% higher calculation time to reach to the same order of numerical convergence as the real gas models. The ideal gas equation of state took about 2.28% lower computational time than the PR and other real gas models.

3.10. R1233zd(E) at 3000 rpm, built-in volume index of 4.5

R1233zd(E) is another low GWP alternative to R245fa (Molés et al., 2014) which has a GWP of 1 and a high safety group rating - A1 in ASHRAE Standard 34, 2010 (Lemmon et al., 2018). Here, the expander was calculated with R1233zd(E) at operating speed of 3000 rpm at 600 kPa pressure and 110.0 °C temperature. The fluid is replaced in the CFD model with its own specific thermodynamic and transport properties. The definition of real gas equation of state follows Eq. (1) to (4) for evaluation of specific volume. In case of R1233zd(E), the zero pressure, ideal gas specific heat c_p^0 , required for the calculation of internal energy and entropy, was also derived from a 4th order polynomial. The critical state temperature and pressure were input to generate a lookup table in the temperature range of 205 and 425 K, while the pressure was set in the range of 25 and 2500 kPa. The input values for the c_p^0 polynomial, the critical point properties, the acentric factor and the molar mass were all taken from REFPROP and Eq. (14) was obtained using them with the reference state values taken as 101.325 kPa, and 25°C. Fluid specific properties for R1233zd(E) were $\omega = 0.3025$, boiling temperature = 291.413 K, $p_c = 36.239$ bar, $T_c = 439.6$ K, $v_c = 273.9726$ cm³ mol⁻¹ and molar mass = 130.4962 kg kmol⁻¹.

$$\frac{c_p^0}{R_s} = c_0 T^0 + c_1 T^1 + c_2 T^2 + c_3 T^3 + c_4 T^4$$

Eq. (14)

$$c_0 = -7.3289348031, c_1 = 1.5082969682e^{-1}, c_2 = -4.6639139859e^{-4}, c_3 = 7.6015634343e^{-7}, c_4 = -4.8307696228e^{-10},$$

Dynamic viscosity and thermal conductivity were specified using the kinetic theory model and critical volume v_c as an input in Eq. (6) and Eq. (7) respectively. For the ideal gas equation of state, a fourth order polynomial as a function of temperature was used for specific heat whose coefficients are obtained from REFPROP at saturation over the temperature range -70.0°C

to 130.0°C. The polynomial coefficients for R1233zd(E) are in Eq. (15) and temperature is in K units.

$$c_p = c_0 T^0 + c_1 T^1 + c_2 T^2 + c_3 T^3 + c_4 T^4$$

$$c_0 = 1.8247558798e^3, c_1 = -2.5518989034e^1, c_2 = 1.7257930074e^{-1}, c_3 = -4.7409600798e^{-4}, c_4 = 4.8532039304e^{-7}$$

Eq. (15)

Table 10 summarises the expander performance as predicted by the CFD model. Compared to R245fa, a higher filling pressure was used for R1233zd(E). It is expected that the flow and power output from the expander will increase thereby increasing the specific power output. The power output is higher at 3.96873 kW with R1233zd(E) as compared to 3.114 kW with R245fa. The specific power of the expander has increased from 12.006 kW kg⁻¹ s with R245fa to 14.573 kW kg⁻¹ s with R1233zd(E). This is due to the higher density of R1233zd(E) that increases the mass flow rate to 0.27234 kg s⁻¹ as compared to 0.25939 kg s⁻¹ with R245fa but the higher filling pressure of 600 kPa increases the power output relatively more. It can be observed from Table 10 that, of the real gas models, RK equation of state has the highest deviation in estimation of flow, power and specific power, it is within 1.0% and practically negligible. The PR, SRK and ARK equation of state are in close agreement with REFPROP with deviation of the order of 0.45%. These can all, therefore, be considered as accurate enough to be used in the selected operating condition of the expander with R1233zd(E). Results using the ideal gas equation of state again deviate significantly from those obtained from REFPROP with differences in flow of 7.81%, indicated power of 4.28% and specific power about 9.95%.

Table 10. R1233zd(E) performance data at 3000 rpm, built-in Vi = 4.5, Inlet Pressure = 600 kPa and Temperature = 110.0°C

Case	R1233zd(E) fluid Data	Flow (kg s ⁻¹)	(%)	Power (kW)	(%)	Specific Power (kW kg ⁻¹ s)	(%)	CPU Time (hr rev ⁻¹)	(%)
1	NIST REFPROP	0.27234	0	3.96873	0	14.573	0	5.95	52.46
2	Redlich Kwong	0.27014	0.81	3.95156	0.43	14.628	0.93	3.83	-1.71
3	Soave Redlich Kwong	0.27170	0.23	3.95532	0.34	14.557	0.41	3.84	-1.60
4	Aungier Redlich Kwong	0.27181	0.19	3.95676	0.30	14.557	0.36	3.83	-1.71
5	Peng Robinson	0.27340	-0.39	3.97576	-0.18	14.542	0.43	3.90	0.00
6	Ideal Gas	0.25106	7.81	3.79906	4.28	15.132	9.95	3.79	-2.78

The recorded CPU time in Table 10 again indicates that REFPROP required about 53% higher calculation time to reach to the same order of numerical convergence as the real gas models. The ideal gas equation of state took about 2.78% lower computational time as compared to the PR and other real gas models.

4. Conclusions

The objective of this analysis was to evaluate computational accuracy in the prediction of expander performance, local variation of fluid properties and the flow solver's computational time requirements when using selected real gas equation of state models instead of REFPROP. For this purpose, a CFD model was developed for a twin screw expander, with the rotor and port grids generated using the SCORG grid generation tool and the ANSYS CFX flow solver with R245fa gas as the working fluid. Results were obtained assuming a main rotor speed of 3000 rpm with 544 kPa filling pressure at 94.26°C and a discharge pressure of 175 kPa. The following observations can be made from the analysis:

- In the operating range of the pressure and temperature at 3000 rpm and Vi 4.5, for R245fa gas, the Peng Robinson equation of state is the most accurate in comparison with the Redlich Kwong, Aungier Redlich Kwong and Soave Redlich Kwong models. The performance results of the expander were identical to those using REFPROP. Local fluid properties such as temperature deviated by less than 3% and the maximum specific volume deviation was 15% in a few local cells present in the leakage gaps.

- The maximum deviation in local temperature between the Redlich Kwong and the Peng Robinson equations from the REFPROP results was 0.86% and maximum deviation in local specific volume was 1.75%.
- Results, using the ideal gas equation of state deviated significantly in the prediction of flow and indicated power. For these parameters, of the real gas models, the RK equation of state has the highest deviation although it is within 1.3% with respect to REFPROP. The PR equation of state gives the closest agreement with a deviation of the order of only 0.3%. The deviation with both the SRK and ARK equation of state is less than 0.6%.
- Close to the critical point (Fig. 1), the use of the Redlich Kwong equation leads to a large deviation in estimates of the pressure and specific volume accuracy compared to those obtained from REFPROP. Hence, the Redlich Kwong equation cannot be used in this operating region. However, its variants the Aungier Redlich Kwong and Soave Redlich Kwong as well as the Peng Robinson models are suitable close to the critical point.
- When using REFPROP to calculate the fluid properties, the CFD solver required more number of sub-iterations per time step to reach the same level of numerical convergence as that of the real gas models. This resulted into the need for a nearly 57% higher computational time requirement.

To further validate the observations from the study, an extended analysis was carried out with varying expander's built-in volume index and operating speed. With a change in V_i , the internal pressure, temperature and specific properties of the fluid will have different variation during the expansion process. With a change in operating speeds, not only the expander's flow and indicated power output changes but also the time step size used in the numerical model has to be changed thus effecting the solver. These variations in the test cases provide useful data for the validity of the observed results. Additionally, low GWP alternative working fluid R290 was evaluated at operating pressure of 600 kPa and temperature of 130.0°C, while R1336mzz(Z) and R1233zd(E) were both evaluated at operating pressure of 600 kPa and temperature of 110.0°C. A larger variety of test cases were thus evaluated, indicated that the real gas equations of state are a suitable alternative to specification of fluid properties in a 3D CFD model under controlled operating conditions. In particular, the expander performance accuracy deviated within practically negligible limits of 0.5 – 2.2% maximum. But on the other hand, a consistent saving in computation time of the order of 43% was achievable.

REFERENCES

- Abdelli, L. 2015. CFD analysis of an expansion process using different real gas models. Masters dissertation, Department of Flow, Heat and Combustion Mechanics. Faculty of Engineering and Architecture. Ghent University, Belgium.
- Aungier, R. H. 1995, A Fast, Accurate Real Gas Equation of State for Fluid Dynamic Analysis Applications, *Journal of Fluids Engineering*, vol. 117 (2), pp. 277–281.
- Bianchi, G., Rane, S., Fatigati, F., Cipollone, R., Kovacevic, A. 2019. Numerical CFD Simulations and Indicated Pressure Measurements on a Sliding Vane Expander for Heat to Power Conversion Applications. *Designs*, 3, 31. doi : 10.3390/designs3030031
- Chung, T. H., Ajlan, M., Lee, L. L., Starling, K. E. 1988. Generalized multiparameter correlation for nonpolar and polar fluid transport properties, *Industrial & Engineering Chemistry Research*, American Chemical Society, SNo 0888 5885, Vol 27, 4, pg 671-679. doi: 10.1021/ie00076a024
- Kovačević, A., Rane, S. 2013. 3D CFD analysis of a twin screw expander. 8th International Conference on Compressors and their Systems. 417-429. Cambridge: Woodhead Publishing. ISBN 9781782421696.
- Kovačević, A.; Rane, S. 2017. Algebraic generation of single domain computational grid for twin screw machines Part II—Validation. *Adv. Eng. Softw.*, 107, 31–43, doi:10.1016/j.advengsoft.2017.03.001.
- Lemmon, E.W., Bell, I.H., Huber, M.L., McLinden, M.O. 2018. NIST Standard Reference Database 23: Reference Fluid Thermodynamic and Transport Properties-REFPROP, Version 10.0, National Institute of Standards and Technology, Standard Reference Data Program, Gaithersburg.

- Molés, F., Navarro-Esbrí, J., Peris, B., Mota-Babiloni, A., Barragan-Cervera, A., Kontomaris, K. 2014. Low GWP alternatives to HFC-245fa in Organic Rankine Cycles for low temperature heat recovery: HCFO-1233zd-E and HFO-1336mzz-Z," *Applied Thermal Engineering*, no. 71, pp. 204-212.
- Papeš, I., Degroote, J., Vierendeels, J. 2015. New insights in twin screw expander performance for small scale ORC systems from 3D CFD analysis. *Applied Thermal Engineering*, 91, 535-546.
- Peng, D., Robinson, D. 1976, A New Two-Constant Equation of State, *Industrial and Engineering Chemistry Fundamentals*, vol. 15 (1), pg. 59–64.
- Poling, B. E., Prausnitz, J. M., O'Connell, J. P. 2001. *The Properties of Gases and Liquids*. Edition 5, ISBN 9780070116825, McGraw-Hill, New York.
- Rane, S.; Kovačević, A.; Stošić, N.; Kethidi, M. 2013. Grid Deformation Strategies for CFD Analysis of Screw Compressors. *Int. J. Refrig.*, vol. 36 (7), 1883–1893. doi: 10.1016/j.ijrefrig.2013.04.008
- Rane, S.; Kovačević, A.; Stošić, N.; Kethidi, M. 2014. Deforming grid generation and CFD analysis of variable geometry screw compressors. *Comput. Fluids*, 99, 124–141. doi: 10.1016/j.compfluid.2014.04.024
- Rane S., Kovačević A. 2017. Algebraic generation of single domain computational grid for twin screw machines. Part I. Implementation. *Advances in Engineering Software*, 107, pp. 38-50. doi: 10.1016/j.advengsoft.2017.02.003
- Redlich, O., Kwong, J. N. S. 1949, On the Thermodynamics of Solutions. V. An Equation of State. Fugacities of Gaseous Solutions, *Chemical Reviews*, vol. 44 (1), pp. 233-244. doi: 10.1021/cr60137a013
- Smith, I. K. 1993. Development of the Trilateral Flash Cycle System: Part 1: Fundamental Considerations. *Proceedings of the Institution of Mechanical Engineers, Part A: Journal of Power and Energy*, 207 (3), pp. 179-194.
- Soave, G. 1972, Equilibrium Constants from a modified Redlich-Kwong equation of State, *Chemical Engineering Science*, vol. 27 (6), pp. 1197-1203. doi: 10.1016/0009-2509(72)80096-4
- Stošić N., Smith I.K. and Kovacevic A. 2005. *Screw Compressors: Mathematical Modelling and Performance Calculation*, Monograph, Springer Verlag, Berlin, ISBN: 3-540-24275-9.